INFECTION AND IMMUNITY, June 2002, p. 2915–2925 Vol. 70, No. 6
0019-9567/02/$04.00+0 DOI: 10.1128/IAI.70.6.2915–2925.2002

Regulation of the Overlapping *pic*/*set* Locus in *Shigella flexneri* and Enteroaggregative *Escherichia coli*

Martin Behrens,† Jalaluddin Sheikh, and James P. Nataro*

Center for Vaccine Development, Departments of Pediatrics, Medicine, and Microbiology & Immunology, University of Maryland School of Medicine, Baltimore, Maryland 21201

Received 20 September 2001/Returned for modification 6 December 2001/Accepted 14 February 2002

Most strains of *Shigella flexneri* 2a and enteroaggregative *Escherichia coli* carry a highly conserved chromosomal locus which encodes a 109-kDa secreted mucinase (called Pic) and, on the opposite strand in overlapping fashion, an oligomeric enterotoxin called ShET1, encoded by the *setA* and *setB* genes. Here, we characterize the genetic regulation of these overlapping genes. Our data suggest that *pic* and the *setBA* loci are transcribed as complementary 4-kb mRNA species. The major *pic* promoter is maximally activated at 37°C in exponential growth phase. Our data suggest that the *setB* gene is transcribed from a promoter which lies more than 1.5 kb upstream of the *setB* structural gene; *setA* may be transcribed via readthrough of the *setB* transcript and possibly by its own promoter. The long leader of the *setB* gene provides a strong silencing effect on *setB* transcription. The signals which provide relief from *setB* silencing are not clear, but significant induction is observed in a continuous anaerobic culture of human fecal bacteria, suggesting that some complex characteristics of the human intestine act to lift repression of *setB* expression. Our studies provide the first insights into the mechanisms affecting expression of this unusual virulence locus.

Shigella flexneri and enteroaggregative *Escherichia coli* (EAEC) are enteric pathogens implicated as agents of diarrheal disease throughout the world. Whereas multiple virulence factors and mechanisms have been elucidated for these organisms, most of the work has focused on plasmid-borne virulence genes. However, several recent studies suggest that genes on the chromosomes of these pathogens are likely to play important roles in pathogenesis (1, 4, 9, 12, 13, 22, 34).

We and others have shown that most *S. flexneri* 2a and EAEC strains share a chromosomal locus, designated *pic*/*set*, which encodes at least two putative virulence factors (1, 4, 9). In *S. flexneri*, *pic*/*set* is encoded on a pathogenicity island called SHI-1 (1); the sequence of the island encoding *pic*/*set* in EAEC has not been reported. *pic*/*set* encodes a high-molecular-weight mucinase (Pic), which is a serine protease secreted by the autotransporter mechanism (12). Pic degrades intestinal mucin and may play a role in mucosal colonization by both EAEC and *S. flexneri* 2a strains. Encoded on the opposite strand but completely within the *pic* gene is an oligomeric enterotoxin called *Shigella* enterotoxin 1 (ShET1), which is thought to comprise a single 20-kDa catalytic A subunit (encoded by the *setA* gene) and five 7-kDa B subunits (encoded by the *setB* gene) (9). The ShET1 mode of action has not been defined, but it does not appear to act via the traditional mediators of toxin-induced intestinal secretion, such as cyclic AMP and cyclic GMP (10).

S. flexneri and EAEC have different pathogenetic strategies. *S. flexneri* is a large-bowel pathogen which causes invasive and inflammatory colitis (for a review, see reference 11). Many shigellosis patients experience a watery prodromal phase, which may be a manifestation of early small-bowel involvement and to which ShET1 may contribute. In contrast, EAEC are thought to be distal small-bowel and/or colonic pathogens which typically cause watery diarrhea without evidence of invasion or frank inflammation (26). Nevertheless, recent data suggest that EAEC may induce mild inflammatory enteritis (31).

We approached the characterization of the *pic*/*set* locus with the aim of understanding when in the pathogenic sequence these loci are expressed and how this expression is controlled. Clarification of these events will provide further understanding of EAEC and *S. flexneri* pathogenesis and may also shed light on signals recognized by enteric pathogens in general. Our data suggest that both loci are expressed in the intestinal lumen; moreover, our results suggest a novel mechanism of ShET1 regulation and the existence of pathogen-specific regulators of *pic* and *setBA*. We also report for the first time the use of a continuous anaerobic culture to study expression of virulence genes.

MATERIALS AND METHODS

Bacterial strains, plasmids, and growth conditions. Strains and plasmids used in this study are listed in Table 1. All *E. coli* strains were grown aerobically at 37°C in Luria-Bertani (LB) medium unless otherwise stated. Antibiotics were added at the following concentrations when appropriate: ampicillin, 100 μg/ml; kanamycin, 50 μg/ml; chloramphenicol, 50 μg/ml, and tetracycline, 50 μg/ml.

Molecular cloning and sequencing procedures. Plasmid DNA purification, restriction, ligation, transformation, and agarose gel electrophoresis were performed by standard methods (28). DNA sequence analysis was performed at the University of Maryland Department of Microbiology & Immunology Biopolymer Facility on an Applied Biosystems model 373A sequencer; template DNA was purified by using minicolumns from Amersham-Pharmacia-Biotech (Piscataway, N.J.).

***lacZ* fusion analysis.** To monitor transcriptional activities, defined fragments from the *pic*/*set* locus were amplified by PCR using primers carrying *Eco*RI and *Bam*HI restriction sites. Fragments were directionally cloned into compatible sites in the promoterless *lacZ* reporter vector pRS551 (30). Clones are listed in Table 1, and primers are listed in Table 2. Cloned fragments were confirmed by

* Corresponding author. Mailing address: 685 W. Baltimore St., Baltimore MD 21201. Phone: (410) 706-5328. Fax: (410) 706-6205. E-mail: jnataro@medicine.umaryland.edu.

† Present address: Limetec Biotechnologies GmbH, 16321 Bernau bei Berlin, Germany.

TABLE 1. Bacterial strains and plasmids used in this study

Strain or plasmid	Genotype or description	Reference or source
Strains		
042	Wild-type EAEC prototype strain	25
E. coli TE2680	K-12 F$^-$/λ$^-$ IN(*rrnD-rrnE*)1 Δ(*lac)X74 rpsL galK2 recD1903*::Tn*10d*-Tet *trpDC700::putPA1303*::[Kan^s-Cam^r-*lac*]	8
E. coli One Shot	K-12 F$^-$ mcrA Δ(*mrr-hsdRMS-mcrBC) ϕ80lacZ*Δ*M15* Δ*lacX74 recA1 deoR araD139* Δ(*ara-leu)7697 galU galK rpsL* (Str^r) *endA1 nupG*	Invitrogen Corp.
E. coli M182	*E. coli* used as background for *hns* and *stpA* mutants; DE(*codB-lac1)3, galK16 galE15* LAM$^-$ e14$^-$ *relA1 rpsL150* (STR^r) *spoT1*	M. Belfort
E. coli M182 *hns*	Kanamycin resistance gene replacing native *hns* gene of *E. coli* M182	M. Belfort
E. coli stpA	Tetracycline resistance gene replacing native *stpA* gene of *E. coli* M182	M. Belfort
042*fis*	042 carrying Tn*phoA* insertion affecting *fis* expression	29a
S. flexneri 2457T	Wild-type *S. flexneri* 2a	6
P3/2	TE2680 ϕ 197-bp fragment with the P*pic*3 promoter::*lacZ*	This study
P15/2	TE2680 ϕ 1,110-bp fragment with the P*pic*1,2,3 promoter::*lacZ*	This study
P16/2	TE2680 ϕ 280-bp fragment with the P*pic*2,3 promoter::*lacZ*	This study
S8/1	TE2680 ϕ 400-bp fragment with the *setA* promoter::*lacZ*	This study
S23/1	TE2680 ϕ 2,755-bp fragment with the *setA* and *setB* promoter::*lacZ*	This study
S23/19	TE2680 ϕ 2,360-bp fragment with the *setB* promoter and the silencer region::*lacZ*	This study
S25/26	TE2680 ϕ 260-bp fragment with the *setB* promoter::*lacZ*	This study
S25/32	TE2680 ϕ 310-bp fragment with the *setB* promoter and 50 bp of the silencer region::*lacZ*	This study
S40/19	TE2680 ϕ 463-bp fragment with the *setB* promoter and 69 bp of the silencer region::*lacZ*	This study
S41/19	TE2680 ϕ 394-bp fragment with the *setB* promoter and the deleted silencer region::*lacZ*	This study
S42/19	TE2680 ϕ 559-bp fragment with the *setB* promoter and 165 bp of the silencer region::*lacZ*	This study
Plasmids		
pRS551	*lacZ* reporter gene fusion vector	Simons
pP3/2	197-bp fragment with the P*pic*3 promoter in pRS551	This study
pP4/2	158-bp fragment without promoter in pRS551	This study
pP15/2	1,110-bp fragment with the P*pic*1,2,3 promoter in pRS551	This study
pP16/2	280-bp fragment with the P*pic*2,3 promoter in pRS551	This study
pP16/20	82-bp fragment with the P*pic*2 promoter in pRS551	This study
pS8/1	400-bp fragment with the *setA* promoter in pRS551	This study
pS12/1	211-bp fragment without promoter in pRS551	This study
pS23/1	2,755-bp fragment with the *setA* and *setB* promoter and the silencer region in pRS551	This study
pS23/19	2,360-bp fragment with the *setB* promoter and the silencer region in pRS551	This study
pS25/26	260-bp fragment with the *setB* promoter in pRS551	This study
pS25/32	310-bp fragment with the *setB* promoter and 50 bp of the silencer region in pRS551	This study
pS40/19	463-bp fragment with the *setB* promoter and 69 bp of the silencer region in pRS551	This study
pS41/19	394-bp fragment with the *setB* promoter and the deleted silencer region in pRS551	This study
pS42/19	559-bp fragment with the *setB* promoter and 165 bp of the silencer region in pRS551	This study
pP37/19	pP16/2 with the 1,562-bp silencer region in the silencing orientation in pRS551	This study
pP37/19inv	pP16/2 with the 1,562-bp silencer region in the inverted orientation in pRS551	This study
pS37/19	pS25/26 with the 1,562-bp silencer region in the silencing orientation in pRS551	This study
pS37/19inv	pS25/26 with the 1,562-bp silencer region in the inverted orientation in pRS551	This study
pPic1	5.7-kbp chromosomal fragment of EAEC 042 in pACYC184	12
pΔ*pic*Ω	pPic1 with deleted P*pic*1,2,3 promoters and the Ω fragment cloned into *Eco*RI restriction site	This study
pΔ*set*	pPic1 with deleted *setA* and *setB* promoters	This study

plasmid isolation and restriction, PCR, and DNA sequencing. β-Galactosidase activity, expressed in Miller units, was measured as described previously (20).

pic, *setA*, and *setBA* promoter regions were integrated into the chromosome of the *E. coli* K-12 strain TE2680 in a single copy as described previously (8). Briefly, the pRS551 plasmid carries a Kan^r gene from Tn*903* placed upstream of the *E. coli lac* operon, separated from *lac* by a transcriptional terminator. Strain TE2680 contains a region homologous to pRS551, comprising a Kan^r gene (which has been inactivated by the insertion of a linker into the *Hin*dIII site) and

TABLE 2. Oligonucleotides used in this study

Application	Primer	Sequence (5′ to 3′)	Strand[a]	5′ end[b]
Fusion constructions	Pic2R*Bam*HI	GGATATGGATCCGTAACACAGACAGATTGCTG	−	1131
	Pic3F*Eco*RI	TATCATGAATTCCTTCAGCTATTTTACTTTTAT	+	934
	Pic4F*Eco*RI	TGTAAAGAATTCGGAGAATCCATAATGAATAA	+	973
	Pic15F*Eco*RI	CATCATGAATTCCGGACGCTTACGAACTGACG	+	21
	Pic16F*Eco*RI	CTCCAGGAATTCCGGGGCGGTTCAGTTCACAA	+	851
	Pic20R*Bam*HI	AAATAGGGATCCAAGCTAATGATAACCCGACGTT	−	933
	Shet1R*Bam*HI	GACCGGGGATCCGGATGTCGCCATTCCACAGG	+	2867
	Shet8F*Eco*RI	CAGCGTGAATTCCCCTTCATACTGGCTCCTGT	−	3267
	Shet12F*Eco*RI	GTCAGCGAATTCCAGCGACAGTGTTTTCATTG	−	3078
	Shet19R*Bam*HI	GGAGCCGGATCCAAGGGAATATTACGCTGAAC	+	3262
	Shet23F*Eco*RI	GAAAGCGAATTCCGCCATGTGCTTGGCGTCAT	−	5622
	Shet25F*Eco*RI	AAACAGGAATTCGCCAGTTGGCAAAACTAGTT	−	5218
	Shet26R*Bam*HI	GATAAAGGATCCAAAGGACAGCCGGATGCTGT	+	4958
	Shet32R*Bam*HI	CTGCTGGGATCCGGAGAGACCGTACTGCGTGA	+	4908
	Shet37F*Bam*HI	TTACCAGGATCCGTCTTGCCCAGTTCAACCCC	−	4838
	Shet40F*Bam*HI	ACCGGCGGATCCATGCCCGTCGCTGAAAAGAC	−	3465
	Shet41F*Bam*HI	CAGTGAGGATCCGGCAAAAGCACCCGGGGCTG	−	3396
	Shet42F*Bam*HI	GGTCAGGGATCCTCCGTCCGTCAGATATACAG	−	3561
RT-PCR	Shet10F	GCCCTGTCACTTCCCAGTGT	−	3170
	Shet13R	CGTAACGCCTCGCTGAACAG	+	3102
	Shet17F	GCAGGGTTGGGGTCACCCGA	−	4138
	Shet20FRT	CGCATATTGTCCTTTATCTG	−	5018
	Shet21FRT	GAAAGGCTGCCTTCCGGCAG	−	5138
	Shet22RRT	TAAGGCCGGCACCCGGGTGA	+	4088
	Shet24FRT	CGATACAAGCGTAGCAACGC	−	1338
	Shet25RRT	TATTGCCCCGTCACCGGGGG	+	1008
	Shet26RRT	ATGGGGGGACTGGCGCAAGC	+	548
	Shet28RRT	CCGGTGAAAACCTGGTATTC	+	2038
	Shet33FRT	GAATACCAGGTTTTCACCGG	−	2058
	Shet34RRT	GCGTTGCTACGCTTGTATCG	+	1318
	Shet35RRT	CTCTAATCCCGGGCAAACTT	+	1688
	Shet36FRT	AAGTTTGCCCGGGATTAGAG	−	1708
Promoter deletions	INVPCR1	TTTTCCTTTTGCGGCCGCCGAGTT AGAGTTTTTTCCAGTATCGATTTT	−	500
	INVPCR2	AAGGAAAAAAGCGGCCGCATGGAG AATCCATAATGAATAAAGTTTATTCTC	+	971
	INVPCR3	TTTTCCTTTTGCGGCCGCGCGAG CCTGTTTAAGATTCTGTGTAAATG	+	5218
	INVPCR4	AAGGAAAAAAGCGGCCGCTCTC CTTTTATCCGTTTCTCCCCGGAC	−	4958
	INVPCR5	TTTTCCTTTTGCGGCCGCAGCCAG TATGAAGGGAATATTACGCTGAAC	+	3252
	INVPCR6	AAGGAAAAAAGCGGCCGCCATA TTCCCGGTCAGCTGACCATGAAAGAT	−	2868
Real-time RT-PCR	RealF	TGTACCTGGTGCCAATGATA	+	1215
	RealRI	CCGATATCCTCCGTTATGCT	−	1380
	RealRII	CGATATACTGAGGCGATACAA	−	1351
	SetARealF	CCCTGATATTCCAGGGACAT	+	2962
	SetARealF	ATGGAAGTCAGCGTCTTTCA	−	3096
	8/1RaceII	GACAGTGGCACCCTGATATT	+	2952
	Shet9F	GGTACCTTCCTCCGGAATGA	−	3225
	SetBReal	CTGAACAGTGACATTAAGTC	+	3114
	Tet1R	TAAGAGCCGCGAGCGATCCT	—[c]	—[c]
	Tet2R	GAGCGATCCTTGAAGCTGTC	—[c]	—[c]
	Tet3F	TGGATGGCCTTCCCCATTAT	—[c]	—[c]
	Real control F	CTGGATATACCACCGTTGATATA	—[d]	—[d]
	Real control I	GGGTGAACACTATCCCATAT	—[d]	—[d]
	Real control II	TCAGGCGGGCAAGAATGTGA	—[d]	—[d]

[a] With respect to the *pic* gene (Fig. 2A).
[b] With respect to Fig. 2A.
[c] Primer for the internal standard (Tc^r gene).
[d] Primer for the internal standard (Cm^r gene).

a downstream segment consisting of the *lac* operon; between these two segments is a Cam^r fragment. TE2680 also bears a *recD*::Tn*10*d-Tet insertion to allow efficient recombination of linearized plasmid DNA. Transformation of 1 μg of linear DNA (cut with *Xho*I) and subsequent recombination yield Kan^r Cam^s recombinants which represent replacement of the TE2680 *lacZ* gene with the chimeric pRS551 derivative (8). Transformants were screened for kanamycin resistance and chloramphenicol sensitivity; integration was verified by PCR prior to β-galactosidase assays.

RNA extraction and RT-PCR techniques. Bacterial strains were grown to exponential phase, and whole-cell RNA was isolated using the RNeasy kit (Qia-

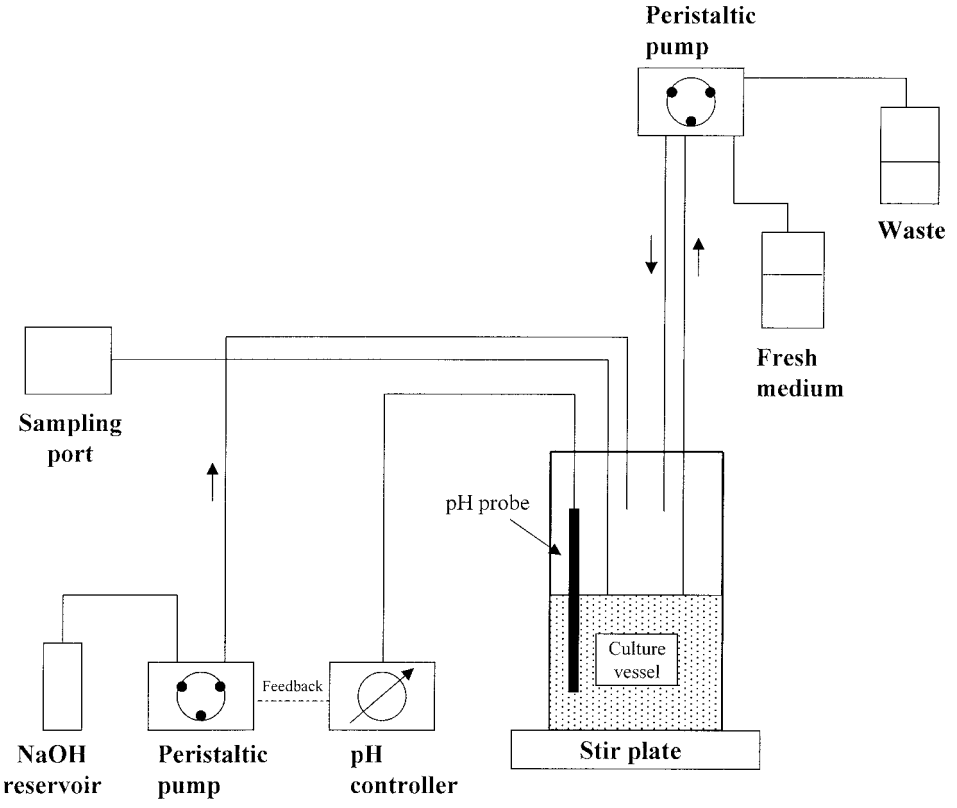

FIG. 1. Diagram of the apparatus used for continuous culture of human fecal bacteria. See Materials and Methods for a detailed description.

gen Inc., Valencia, Calif.) according to the manufacturer's instructions. RNA was treated with RNase-free DNase to eliminate contaminating DNA. cDNA was synthesized using sequence-specific primers (Table 2) and the Superscript enzyme from Gibco-BRL (Gaithersburg, Md.) for 10 min at 55°C. PCR was performed using standard procedures with *Taq* DNA polymerase (BRL). Controls for all reactions included samples without reverse transcriptase (negative control) and the relevant purified plasmid DNA (positive control).

The abundance of mRNA transcripts for *pic* and *set* genes was determined by real-time quantitative reverse transcription (RT)-PCR. RNA extracted as above was tested for DNA contamination by 40 cycles of standard PCR with the same primers used in the RT-PCR amplification. Single-step RT-PCR was performed with the Superscript enzyme in the presence of SYBR Green I dye (Roche Molecular Biochemicals, Mannheim, Germany), followed by PCR performed according to the manufacturer's instructions using AmpliTaq Gold polymerase (Roche). Fluorescence was detected with the GeneAmp 5700 sequence detection system and accompanying software. The threshold for positivity was set at 1. The constitutively expressed *cat* (chloramphenicol acetyltransferase) gene of *E. coli* O42 was used as an internal standard for reactions involving this strain; the *tet* gene of pACYC184 was used as the standard for experiments involving pPic1. For each primer pair, a standard curve was generated by using known amounts of purified *pic*/*set* plasmid pPic1 (12). Unless otherwise indicated, experiments were performed with exponential-phase cells grown in L-broth.

Simulated human intestinal microbial ecosystem. The simulated intestinal ecosystem was essentially that described in references 7 and 21, with the modifications described below (Fig. 1). The system comprised a continuous anaerobic culture of human feces maintained for at least 8 days at 37°C and pH 6.9 (Fig. 1). The growth medium of the culture has been shown previously to provide a stable culture of colonic bacteria and is designed to mimic the conditions of the human transverse colon (Table 3) (21). The volume of the culture was 500 ml, and flow was set to provide turnover of 1 culture volume/24 h. The inoculum consisted of 50 g of fresh feces, which was preincubated in 100 ml of fermentor medium for 6 h with stirring. Thereafter, 60 ml of this starter culture was inoculated into the main fermentor culture. The fecal inoculum was cultured quantitatively for aerobic and anaerobic bacteria as described in reference 32.

The culture in the fermentation vessel (Lofstrand Bactolift, 1 liter; Lofstrand Inc., Gaithersburg, Md.) was stirred continuously at 100 rpm by a magnetic stirrer. pH was monitored continuously by means of an electrode inserted through a port in the lid; the pH meter (Cole-Parmer Instruments, Vernon Hills, Ill.) was servocontrolled and maintained the desired setpoint by on-demand dispensation of 4 M NaOH via a peristaltic pump. Fresh medium was introduced into the culture vessel from a 2-liter reservoir by peristaltic pump. To help prevent retrograde bacterial growth, the medium was stored at pH 2. The entire system was maintained at a constant temperature of 37°C.

After the fermentor had been stabilized for at least 7 days, a sample was withdrawn and cultured again quantitatively for aerobic and anaerobic flora. Only if the bacteriologic profile was similar to that of the fecal inoculum was the experiment continued.

To study gene regulation in the fermentor, *E. coli* 042 harboring different *lacZ* fusion plasmids was introduced into the fermentation vessel. The preinoculation baseline β-galactosidase activity of the culture in the fermentation vessel was

TABLE 3. Medium used for intestinal simulation cultures[a]

Compound	Concn
NaCl	30 mmol/liter
$NaHCO_3$	5 mmol/liter
KCl	5 mmol/liter
Bacto-Peptone (Difco)	5 g/liter
Mucin (Sigma)	2.5 g/liter
Starch	0.6 g/liter
Glucose	2.5 g/liter
Maltose	3 g/liter
Hemin	1×10^{-4} g/liter
Thioglycolic acid	4.5 mmol/liter

[a] Modified from reference 21.

determined at steady state. This value was subtracted from all subsequent measurements. An overnight culture of *E. coli* 042 harboring a pRS551 *lacZ* fusion construct was then introduced into the fermentation vessel to an initial concentration of 5×10^6 CFU/ml, and the β-galactosidase activity was immediately sampled after mixing (time zero). The third and final measurement was carried out after 24 h of incubation. The number of *E. coli* 042 CFU was determined at time zero and after 24 h of incubation by plating dilutions on LB-agar plates containing ampicillin (100 μg/ml); cultures from the fermentation vessel without added *E. coli* 042 did not yield growth on these plates. Miller units were calculated according to the standard equation (20), except that the number of 042 CFU was converted to an optical density at 600 nm (OD_{600}) value at the ratio of 1 $OD_{600} = 10^9$ CFU, determined to have a protein concentration of 0.2 μg/ml.

RESULTS

Transcriptional organization of *pic* and *set* genes. The *pic*/*set* loci from *S. flexneri* 2a strain 2457T and EAEC strain 042 were cloned and sequenced previously (12). Both sequences comprise the *pic* structural gene of 4,116 nucleotides and, on the complementary strand, the *setA* gene (534 nucleotides) and the *setB* gene (186 nucleotides) (Fig. 2A). The loci from the two strains are 99% identical.

Sequence analysis suggests that upstream and downstream of *pic* lie insertion sequence-like elements (coordinates 275 to 496 and 5536 to the end in Fig. 2A), suggesting that transcription does not occur as part of a larger polycistronic message. This inference was confirmed by using RT-PCR: primers upstream or downstream of the *pic* structural gene did not generate products in RT-PCRs when paired with primers internal to the *pic* structural gene (not shown).

In contrast to *pic*, sequence analysis did not provide clues as to the likely start sites for *setB* or *setA* transcription. When subjected to RT-PCR analysis (Fig. 2) with a series of overlapping primer pairs from the upstream region of the *set* strand, only primer pair 21FRT and 22RRT failed to yield a product; these data suggest that the most upstream *setB* transcription start site lies between coordinates 4958 (the position of primer 20FRT) and 5218 (the position of primer 21FRT) in Fig. 2A, i.e., at least 1.6 kb upstream of the *setB* start codon and downstream of the *pic* stop codon on the opposite strand. Interestingly, of the *setA* downstream primers, only 26RRT failed to generate a product when paired with any other primer. This experiment suggests the presence of a transcriptional terminator of *set* mRNA upstream of the *pic* start codon on the opposite strand. Moreover, our RT-PCR data using overlapping primers suggested the presence of a *setBA* polycistronic mRNA, since primer pair 35RRT and 33FRT span the junction of the two open reading frames (ORFs).

RT-PCR experiments thus directed us toward the flanking regions of *pic* as the likely location of promoters for both *pic* and *set,* albeit on opposite strands. Primer extension experiments of the *pic* gene using automated sequencing protocols produced multiple potential start sites, without any clearly preferred site. One potential start site corresponded to the previously predicted σ^{70} promoter 19 bp upstream of the *pic* start codon (12), but additional potential sites were found upstream.

To better characterize the *pic* promoters, we cloned a series of *pic* upstream DNA fragments into the multiple cloning site of promoterless *lacZ* reporter vector pRS551 (Fig. 3) and electroporated the plasmids into EAEC strain 042. Three regions of interest were designated $P_{pic}1$ (between coordinates 21 and 851 of Fig. 3), $P_{pic}2$ (between coordinates 851 and 933), and $P_{pic}3$ (between coordinates 934 and 1131 and including the predicted promoter from reference 12). The transcriptional start site suggested by RT-PCR mapped between coordinates 537 and 693, within the $P_{pic}1$ region. However, *lacZ* fusion data suggested that this promoter was weak under the conditions tested (compare pP15/2 and pP16/2 in Fig. 3). Fragment $P_{pic}2$ yielded the highest *lacZ* expression levels, yet, a *lacZ* reporter fusion with $P_{pic}2$ alone (pP16/20) yielded threefold less β-galactosidase activity than a fusion including both the $P_{pic}2$ and $P_{pic}3$ regions (pP16/2). A fusion construct comprising only $P_{pic}3$ (pP3/2) yielded 20-fold-higher activity than a construct that did not include any of the predicted promoter regions (pP4/2). A fusion construct comprising only the $P_{pic}1$ region (21 to 851) yielded ninefold higher activity than pRS551 alone (not shown in the figure). These data suggest that multiple promoters direct *pic* expression.

lacZ fusion experiments suggested the presence of a weak promoter just upstream of *setA*, between coordinates 2867 and 3267 in Fig. 3. This putative promoter was designated P_{setA}. No promoter activity was identified immediately upstream of *setB*. We therefore constructed a series of nested fragments of the *setB* upstream region as fusions in pRS551; these fragments extended from immediately upstream of *setB* to the *setB* transcriptional start site suggested by RT-PCR analyses. Among the *setB* fusions, plasmid pS25/26, comprising only the region downstream of the *pic* stop codon (coordinates 4958 to 5218), showed the highest β-galactosidase activity (1,651 Miller units); this activity was only observed when the fragment was cloned in the same orientation as *setBA* (i.e., the *pic* antisense orientation). We designated the promoter in this region P_{setB}.

Surprisingly, DNA fragments comprising the predicted P_{setB} promoter but also including additional downstream DNA suggested the presence of a repressing downstream regulatory element (DRE) or silencer region. A series of *lacZ* fusion constructs localized the *setB* DRE between positions 4958 and 3396 (Fig. 3). Analyzing a further series of deletions in the predicted DRE, we found that even small segments (ca. 50 to 60 bp) of this element extending to either end were sufficient to repress P_{setB} activity. The deletion of the entire predicted DRE (pS41/19) restored P_{setBA} activity almost to the levels exhibited by pS25/26.

Since all of the above fusions were constructed in high-copy-number plasmid pRS551, we transferred the *lacZ* fusions onto the chromosome of the *E. coli* K-12 strain TE2680 in single copy. The relative activities of the different fusions integrated into the TE2680 chromosome were similar to the activities observed in the extrachromosomal constructs (Fig. 3). These experiments suggest that our data were not influenced by copy number or topologic effects.

Orientation-specific regulation of *pic* and *set* genes by *set* silencer region. Given that the *setB* DRE is embedded within the *pic* sequence, we asked whether the *set* silencer acted only on the *set* strand or instead bidirectionally, thereby also silencing *pic* expression. The *lacZ* reporter fusion plasmids pP16/2 (comprising $P_{pic}2,3$) and pS25/26 (P_{setB}) were used in these experiments. The silencer region was amplified by PCR and cloned in both orientations downstream of $P_{pic}2,3$ or P_{setB}. Results of β-galactosidase assays for all four constructs are shown in Fig. 4.

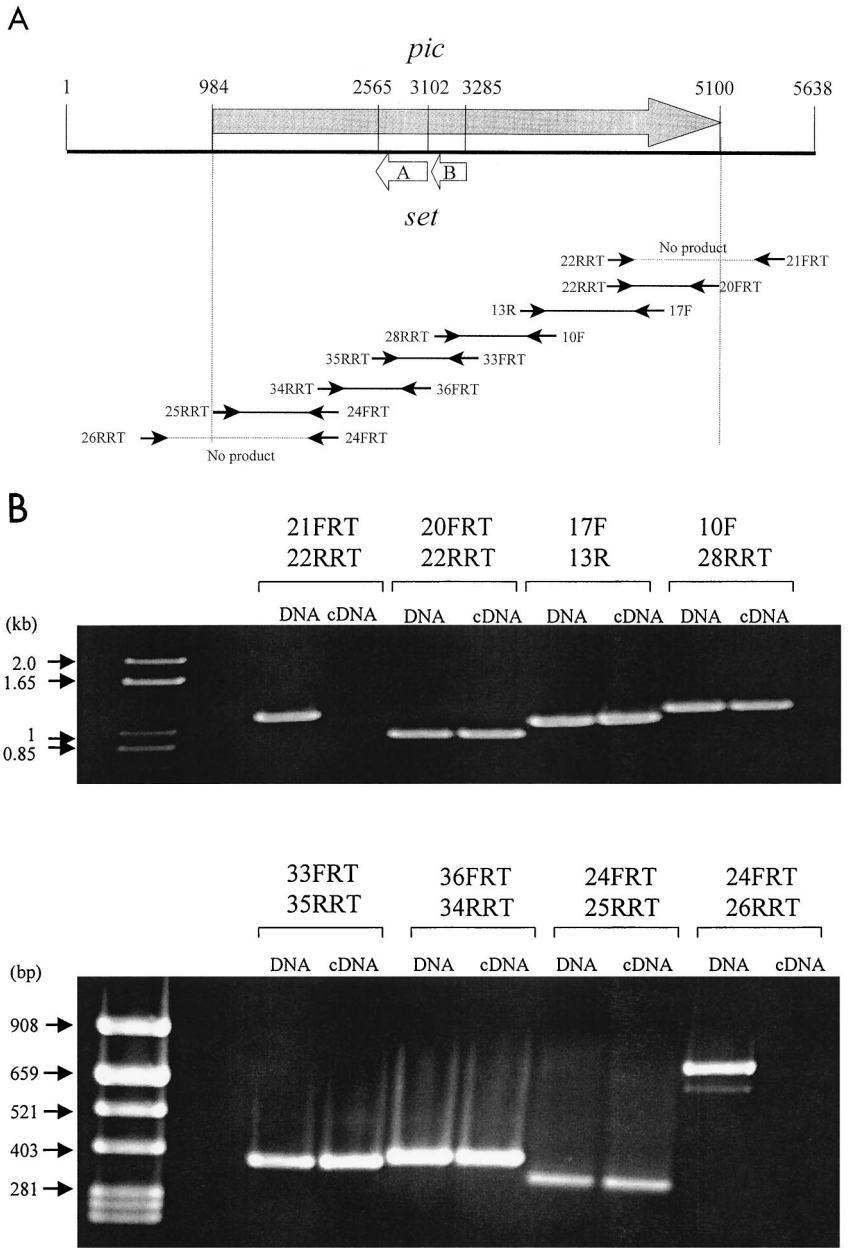

FIG. 2. Organization of the *pic*/*set* locus. (A) Map of the chromosomal DNA fragment encoding *pic* and *setBA* and results of RT-PCR experiments to determine the initiation and termination sites of *set* transcription. Locations of nested *set* primers are indicated, along with presence (solid line) or absence (dotted line) of product generated by that primer pair. (B) Agarose gel electrophoresis demonstrating products of RT-PCR from the *pic*/*set* locus, using the primers illustrated in panel A. RNA was extracted from EAEC strain 042 and subjected to RT synthesis and cDNA amplification by standard PCR (cDNA lanes). A direct PCR step was carried out in parallel on 042 DNA to demonstrate the specificity of the PCR (DNA lanes). The primer pairs used are shown above the lanes. Molecular size markers are shown in the first lane of each gel; the sizes of some markers are indicated.

As predicted, the silencer in the native orientation downstream of the *setB* promoter yielded low β-galactosidase activity. However, inversion of the silencer downstream of P_{setB} derepressed transcription by 46-fold. The silencer cloned in the inverted orientation (compared with the native) downstream of $P_{pic}2,3$ repressed transcription from the *pic* promoters by 14-fold. As expected, the silencer in the native orientation did not have any repressing effect on *pic* transcription. These results suggest that the silencer region represses transcription from either P_{setB} or $P_{pic}2,3$ in an orientation-specific manner.

Conditions affecting regulation of *pic* and *set* transcription. We sought to identify conditions under which *pic* and *set* were maximally expressed. We tested *lacZ* expression of fusions pP15/2 ($P_{pic}1,2,3$) and pS23/19 (P_{setB} with silencer) under the following conditions: carbon starvation, anaerobiosis, iron limitation, and adherence to plastic, as well as varied pH, osmo-

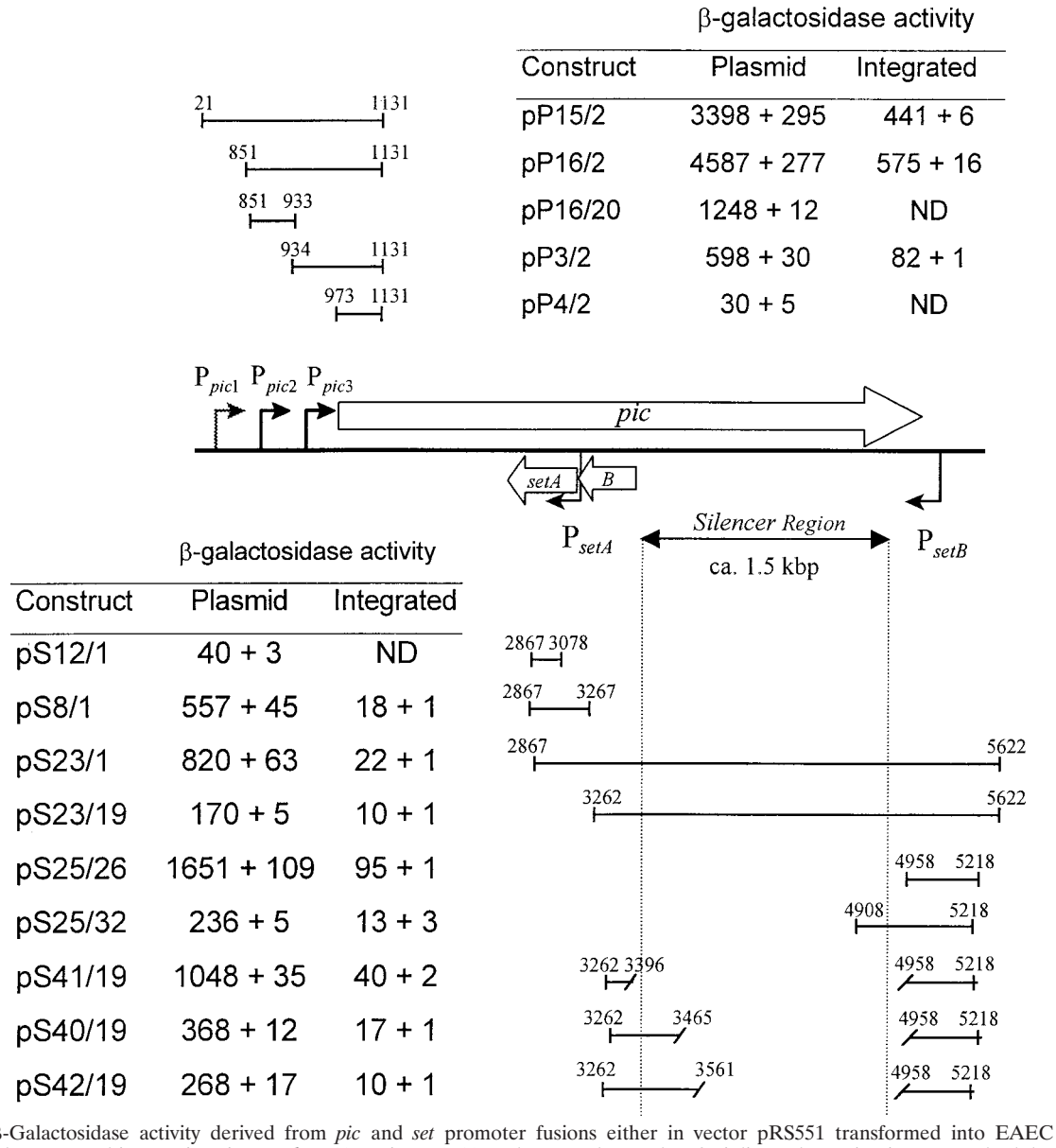

FIG. 3. β-Galactosidase activity derived from *pic* and *set* promoter fusions either in vector pRS551 transformed into EAEC 042 or as single-copy chromosomal integrations in *E. coli* K-12 strain TE2680. Values are the results of triplicate determination + standard deviation. The plasmids are described in Table 2. The numbers above the inserts refer to nucleotide positions with respect to Fig. 2. *pic* fusions are expressed from left to right and *set* fusions from right to left with respect to the *lacZ* gene. ND, not determined.

larity, temperature, and growth phase. None of the conditions yielded P_{setB} activity significantly higher than that in the negative control, whereas a baseline level of *pic* expression was observed in all conditions at 37°C. Only logarithmic growth phase produced any detectable increase in *pic* expression over baseline (data not shown).

To characterize further the effect of growth phase in the EAEC strain 042 background, we employed real-time quantitative RT-PCR for *pic* and *setBA* transcripts. Whole-cell RNA was isolated from strain 042 at three time points after nutrient upshift (0.5, 1.5, and 6.5 h), and cDNA was synthesized as the template for quantitative RT-PCR. For the *pic* gene, we detected clear growth phase-dependent expression (Fig. 5A). However, the abundance of the *setBA* transcript displayed no significant change during growth, confirming that different signals are likely to be responsible for regulation of the *pic* and *setBA* genes.

We next used the *lacZ* reporter gene fusions pP15/2 (P_{pic}1,2,3), pP16/2 (P_{pic}2,3), and pP3/2 (P_{pic}3) transformed into *E. coli* 042 to determine which of the potential *pic* promoter regions were sensitive to growth phase-dependent regulation. As illustrated in Fig. 5B, only promoter P_{pic}2 appeared to be regulated by growth, exhibiting nearly fivefold induction between 0.5 and 1.5 h after nutrient upshift. The construct carrying P_{pic}3 alone yielded a modest activation (less than twofold) between 0.5 h and 1 h, and P_{pic}1 exhibited no detectable growth phase-dependent increase.

From these studies, we infer that (i) region P_{pic}1 is weak

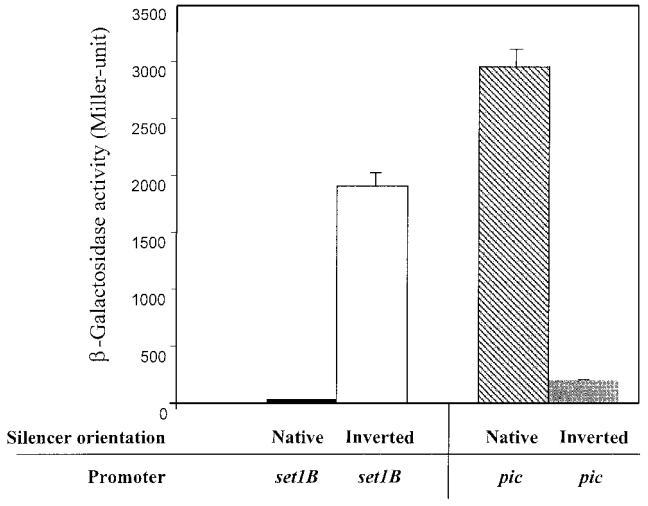

FIG. 4. DNA strand-specific regulation of the *pic* and *set* genes by the *set* DRE silencer region. Results represent β-galactosidase measurements of at least triplicate determinations from L-broth cultures grown to late logarithmic phase; error bars represent 1 standard deviation. Test strains were EAEC strain 042 transformed with *pic* or *set* promoter DNA cloned upstream of the *lacZ* reporter in plasmid pRS551. Constructs used in these experiments were pS37/19 (*setB* promoter with the silencer in the native orientation); pS37/19-inverted (*setB* promoter with the silencer in the inverted orientation), pP37/19 (P_{pic}2,3 promoter region with the silencer in the native orientation), and pP37/19-inverted (P_{pic}2,3 promoters with the silencer in the inverted orientation).

under all conditions tested, (ii) P_{pic}2 harbors a strong promoter inducible during growth, and (iii) the promoter within P_{pic}3 may be constitutively expressed but at low levels. These observations suggest that the P_{pic}2 promoter is the major source of *pic* expression.

Notably, we were unable to identify any in vitro conditions that induced expression of *setB*. Since silencing in *E. coli* typically involves binding of a histone-like protein to a DRE (3, 5, 14, 16, 18, 27, 35–38), we analyzed *lacZ* expression from construct pS23/19 (P_{setB} with silencer) in *E. coli* K-12 strains carrying known mutations in Fis, H-NS, or the H-NS homolog StpA. *lacZ* expression was not derepressed in any of these mutants compared with the *E. coli* K-12 parent (not shown).

Regulation of *pic* and *set* genes in EAEC, *E. coli* K-12, and *S. flexneri*. Maurelli et al. have reported that *Shigella* strains have undergone a large chromosomal deletion which results in augmentation of enterotoxic effects (19). This observation could be mediated in part by different regulatory controls of ShET1 operative in nonpathogenic *E. coli* versus *Shigella* spp. To address this hypothesis, *lacZ* reporter fusions with P_{pic}1,2,3 (pP15/2), P_{pic}2,3 (pP16/2), P_{pic}3 (pP3/2), P_{setB} (pS25/26), P_{setB} with the full silencer region (pS23/19), and P_{setA} (pS8/1) were transformed into EAEC strain 042, *E. coli* K-12, and *S. flexneri* 2457T (Fig. 6).

Expression of *pic* from all promoter constructs was not significantly different between the pathogens EAEC and *S. flexneri*. However, *pic* expression in both the EAEC and *Shigella* backgrounds was substantially higher than in *E. coli* K-12 (at least fivefold higher for both P_{pic}1,2,3 and P_{pic}2,3 fusions). Similarly, expression of P_{setB} and P_{setA} promoters was slightly higher in *S. flexneri* than EAEC, but was higher in both backgrounds than in *E. coli* K-12. However, the silencing effect of the P_{setB} DRE was similar in all three backgrounds.

Regulation of *setB* transcription in a simulated human intestinal microbial ecosystem. Using conventional approaches, we were not able to identify in vitro conditions or mechanisms that resulted in relief of P_{setB} silencing. We therefore expected either that the DRE was continually repressed, providing constitutively low levels of the ShET1 toxin, or that the bacterium

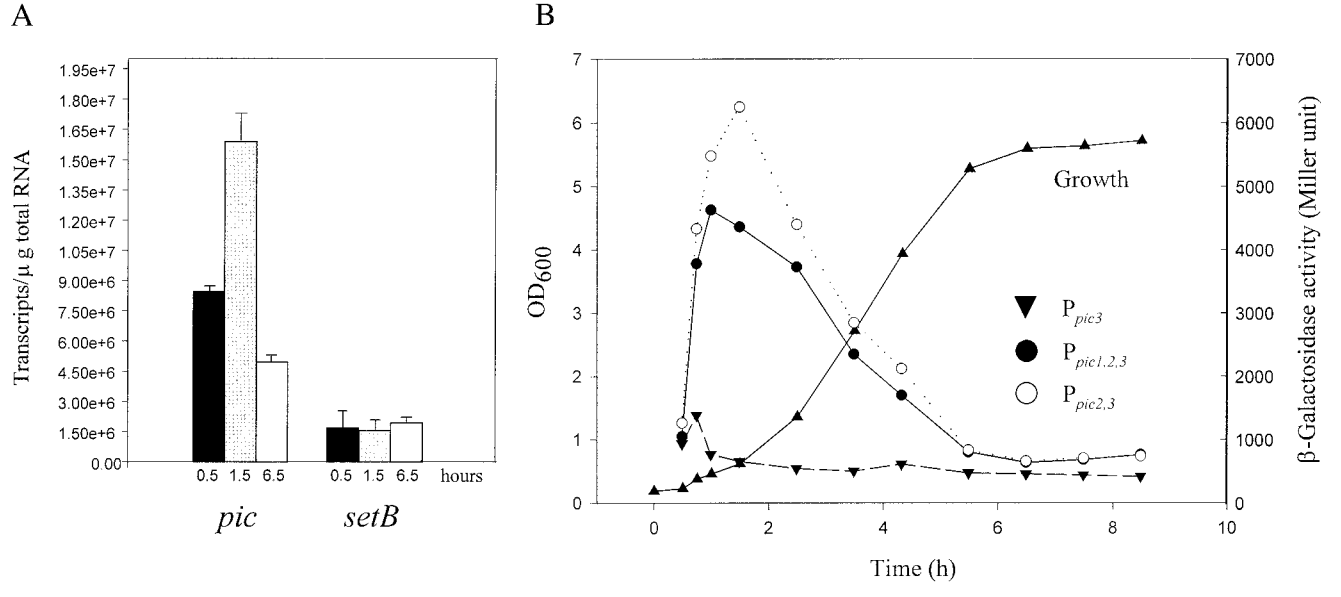

FIG. 5. (A) Effect of growth phase on *pic* and *set* expression as determined by real-time quantitative RT-PCR. RNA was extracted from *E. coli* 042 grown in L-broth for various times (0.5, 1.5, and 6.5 h) after 1:20 dilution of an overnight culture with fresh medium. cDNA was synthesized and subjected to quantitative RT-PCR as described in Materials and Methods. (B) β-Galactosidase activity of *E. coli* 042 harboring plasmid pP15/2 (P*pic*1,2,3), pP16/2 (P*pic*2,3), or pP3/2 (P*pic*3) grown in L-broth and assayed at various times after dilution of overnight cultures with fresh medium.

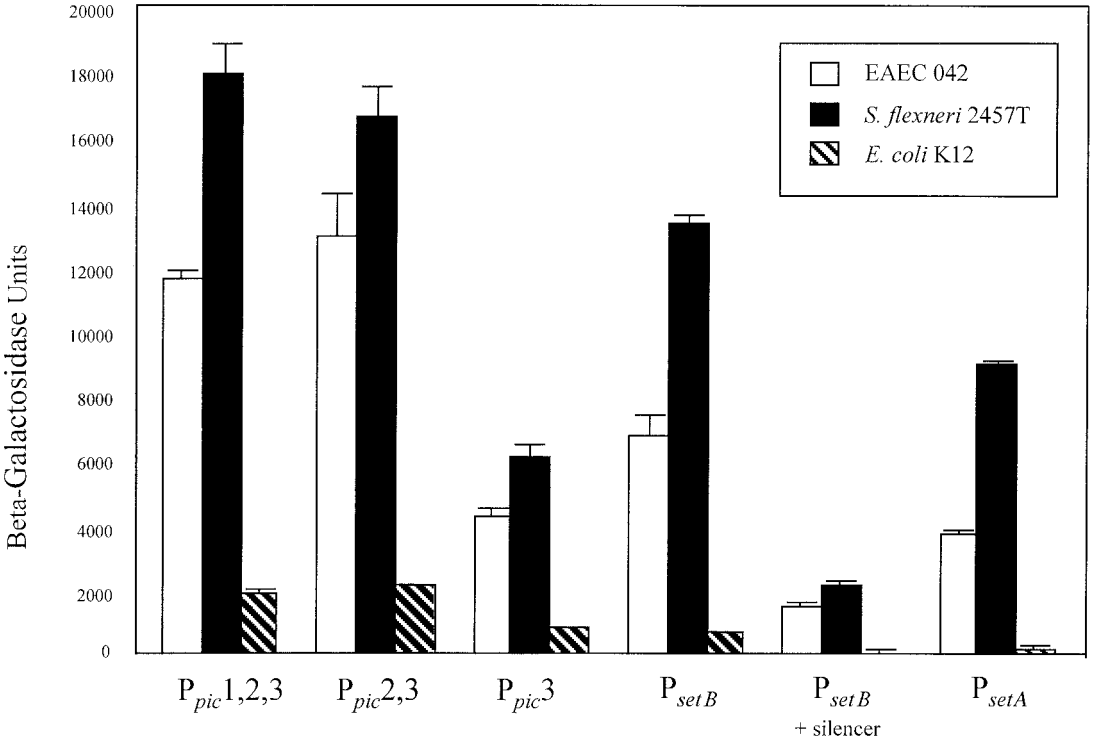

FIG. 6. Transcriptional regulation of *pic* and *set* in EAEC strain 042, *E. coli* K-12, and *S. flexneri* 2457T. Plasmids containing all three *pic* promoter regions (P_{pic}1,2,3), two *pic* promoter regions (P_{pic}2,3), the most downstream *pic* promoter region (P_{pic}3), the *setB* promoter (P_{setB}), the *setB* promoter with the DRE silencer region, or the *setA* promoter (P_{setA}) constructed in pRS551 were transformed into EAEC 042, *S. flexneri* 2457T, or *E. coli* K-12 and tested for β-galactosidase activity. Bacterial strains were grown to exponential phase in L-broth medium at 37°C to the late logarithmic phase. Bars represent results of at least three determinations; error bars represent 1 standard deviation.

would respond to some in vivo signal to induce toxin expression.

Given that no good animal models are available for either *Shigella* or EAEC infection, we tested our hypothesis in a simulated human intestinal ecosystem. Continuous-flow anaerobic cultures have been used previously to study the ecology of the complex intestinal ecosystem (7, 21). Adapting these published protocols, we established such a continuous anaerobic culture, inoculated with fecal material from healthy humans. The baseline β-galactosidase activity in the fermentor was determined before adding the test strain; the test strain, EAEC strain 042 harboring a *lacZ* reporter construct, was added to the vessel, and β-galactosidase activity was measured again. The last β-galactosidase determination was performed 24 h after addition of the test strain. Results are reported in Table 4.

When we introduced 042(pS23/19) into the simulator, the activity of the *setB* promoter, including its DRE, was increased up to 54-fold. In contrast, the same strain grown anaerobically in LB exhibited low β-galactosidase activity. Strain 042(pS23/19) grown aerobically in the simulator medium yielded low reporter activity. EAEC strain 042 transformed with the *lacZ* reporter plasmid (pRS551) alone did not show an increase in β-galactosidase activity in the fermentor (data not shown). Construct pS25/26, expressing only the P_{setB} promoter without the silencer, likewise did not show increased expression in the simulator, suggesting that relief of silencing was the dominant effect of the simulated intestinal environment.

DISCUSSION

The mucinase Pic and *Shigella* enterotoxin 1 are recently described factors which may play important roles in the virulence of *S. flexneri* 2a and EAEC. Whereas recent research has characterized aspects of the pathogenetic schemes for both of these pathogens, significant questions remain. Among these questions is the mechanism of the watery diarrhea phase seen in many cases of shigellosis. In addition, it is notable that *S. flexneri* 2a is the single most prevalent *Shigella* species worldwide (17); the mechanism for this increased virulence or transmissibility is not known, but the presence of *pic*/*set* in this serotype is one possible explanation.

In this study, we have characterized the transcriptional regulation of the *pic* and *set* genes on the complementary strands in *S. flexneri* strain 2457T and EAEC strain 042. Although the

TABLE 4. Activation of *setB* promoter in the simulated human intestinal microbial ecosystem[a]

Growth conditions	Mean β-galactosidase activity (Miller units) ± SD	Mean fold induction ± SD
Simulator (anaerobic)	44,290 ± 12,458	54 ± 15
Simulator medium (aerobic)	299 ± 31	0.4 ± 0.1
LB medium (anaerobic)	819 ± 166	1 ± 0.2

[a] The test strain for all experiments was 042 (pS23/19). Results are means and SDs for three experiments. Fold induction represents β-galactosidase levels at 24 h compared with levels at time zero (time of inoculation of the culture).

major promoter could not be assigned with certainty, the region upstream of *pic* yielded multiple fragments with promoter activity, and overall expression of *pic* was highest in the exponential growth phase. Promoter region $P_{pic}3$ contains a predicted σ^{70} promoter and increases *lacZ* expression in several different constructs, but with only slightly increased expression in exponential phase. Region $P_{pic}2$ does not contain a strongly predicted σ^{70} promoter, but it does confer strong growth phase-dependent *lacZ* expression in a reporter vector. RT-PCR suggests the presence of a transcript starting further upstream ($P_{pic}1$), and expression in a promoter-screening vector suggests that there is a functional promoter in this region as well. In toto, these observations suggest that the nutrient upshift and favorable temperatures experienced by the bacteria upon entry into the human intestine may induce *pic* expression from the major promoter, making the mucinase available at an early stage of the infection. It is possible that a second promoter (possibly $P_{pic}3$) ensures a constitutive low level of the mucinase, perhaps to facilitate the acquisition of nutrients once the bacterium is embedded within the mucus layer.

Expression studies of *setBA* yielded several surprises. Our RT-PCR data were most consistent with the existence of a ca. 4-kb transcript which encodes both *setA* and *setB.* We were not, however, able to demonstrate the existence of such a transcript by Northern blot, most likely because of the weak expression levels observed during in vitro growth. *setA* expression may initiate from a promoter immediately upstream of the structural gene or by readthrough from the *setB* promoter.

We found it notable that the strongest *setB* promoter was located at a site downstream of the *pic* stop codon on the opposite strand and that transcription from P_{setB} is silenced by a DRE. Well-characterized examples of such a downstream prokaryotic silencer have been reported for the *proU* operon of *Salmonella enterica* serovar Typhimurium (27), the *hly* operon of *E. coli* (15), the *bgl* promoter of *E. coli* (29), and the *coo* operon of enterotoxigenic *E. coli* (24). For *proU* and *hly*, the DRE spans some 200 bp, while for *coo*, the DRE is at least 900 bp long. The size of the *bgl* DRE has not been determined precisely. At 1,562 bp (by our definition), the DRE of the *set* operon would be the largest prokaryotic DRE yet delimited. We have also demonstrated that the *setB* DRE is orientation specific; only transcription starting from the *setB* promoter is silenced, whereas transcription of the *pic* gene is not repressed in the native orientation. On the other hand, inversion of the DRE leads to silencing of *pic* and not *setB*. In contrast, the *bgl* DRE can be inverted without impairing its activity (29). Also notably, the *proU* silencer does not regulate the *tac* promoter when cloned in a downstream position (27), whereas the *bgl* silencer is able to repress other promoters (*lac* and *lacUV5*).

The *E. coli* histone-like proteins Fis, H-NS, and StpA are apparently not individually responsible for the silencing effect of the *setB* DRE. This was surprising, since Fis and/or H-NS is essential for silencing of *proU* (27), *bgl* (29), and *coo* (2, 23, 24, 33). It is possible that these histone-like proteins may need to act in concert at the *setB* DRE or that another mechanism may be involved. Deletions which retained small portions from either end of the *setB* silencer region resulted in effective repression; only complete deletion of the region yielded relief of the repressed phenotype. The ability of small DNA regions to effect repression strongly argues against silencing by virtue of an RNA or DNA secondary structure.

We sought to identify in vitro conditions that relieved *setB* silencing, principally to suggest the timing of *set* expression in vivo. Surprisingly, were unable to do so by conventional methods. We therefore employed a novel approach which provides multiple in vivo-like conditions simultaneously, including temperature, pH, osmolarity, low oxygen tension, mucin, and the presence of quorum-sensing signals. We found that *setB* silencing was relieved (i.e., increased up to 54-fold) in a fermentor simulating the human intestine. The precise set of signals provided by the simulator are not so far apparent. Simulated human intestinal microbial ecosystems have been described by several groups (7, 21), but to our knowledge the simulator has not been used previously to study gene regulation.

Use of a simulated intestinal environment offers a number of obvious advantages in the study of gene regulation. The fermentor allows exposure of the pathogen to multiple conditions that are likely to be encountered in vivo. Just as importantly, the simulator can be modified to dissect the critical signals by removing or altering characteristics singly or in combination. The system is also more easily manipulated and sampled than an animal model, and significantly, the system can be tuned to the conditions of the human intestine, thereby avoiding erroneous observations drawn from interspecies variation in the flora or other conditions of the intestine. Further characterization of the expression of *pic*, *set*, and other virulence genes in the simulator is under way.

Although the *pic* and *set* loci are nearly identical in *S. flexneri* and EAEC, previous data suggest that the ShET1 toxin is more active in *Shigella* spp. Maurelli et al. have suggested that this observation is due to the deletion of a large region of the *Shigella* chromosome (the so-called black hole), which results in enhanced enterotoxic effects (19). These authors have suggested further that cadaverine, a product of the lysine decarboxylase reaction, may directly inhibit toxin activity. Our data suggest that the expression of the *set* genes may be enhanced in *Shigella* spp. and EAEC compared with *E. coli* K-12. Whether this effect is due to the loss of a negative regulator encoded on the black hole or to the presence of an additional pathogen-specific activator is not yet clear.

Our studies have characterized a novel locus in *S. flexneri* 2a and EAEC. It has not escaped our notice that additional virulence genes could be encoded by the *setB* mRNA. Indeed, two potential ORFs (>50 amino acids) are found within the DRE region; these are currently being characterized. Further studies to elucidate the roles of *pic*/*set* will likely provide new insights into the pathogenesis of *Shigella* spp. and EAEC.

ACKNOWLEDGMENTS

This work was supported by U.S. Public Health Service awards AI33096 and AI43615 to J.P.N.

We are grateful to Marlene Belfort for bacterial strains and Nicholas Carbonetti and Jay Mellies for critical review of the manuscript. We acknowledge the excellent technical assistance of Suzanne Davis and Thomas J. Maher III.

REFERENCES

1. **Al-Hasani, K., K. Rajakumar, D. Bulach, R. Robins-Browne, B. Adler, and H. Sakellaris.** 2001. Genetic organization of the *she* pathogenicity island in *S. flexneri* 2a. Microb. Pathog. **30:**1–8.

2. **Caramel, A., and K. Schnetz.** 2000. Antagonistic control of the *Escherichia coli bgl* promoter by FIS and CAP in vitro. Mol. Microbiol. **36:**85–92.
3. **Claret, L., and J. Rouviere-Yaniv.** 1996. Regulation of HU alpha and HU beta by CRP and FIS in *Escherichia coli.* J. Mol. Biol. **263:**126–139.
4. **Czeczulin, J. R., T. S. Whittam, I. R. Henderson, F. Navarro-Garcia, and J. P. Nataro.** 1999. Phylogenetic analysis of enteroaggregative and diffusely adherent *Escherichia coli*. Infect. Immun. **67:**2692–2699.
5. **Drlica, K., and J. Rouviere-Yaniv.** 1987. Histonelike proteins of bacteria. Microbiol. Rev. **51:**301–319.
6. **DuPont, H. L., M. M. Levine, R. B. Hornick, and S. B. Formal.** 1989. Inoculum size in shigellosis and implications for expected mode of transmission. J. Infect. Dis. **159:**1126–1128.
7. **Edwards, C. A., B. I. Duerden, and N. W. Read.** 1985. Metabolism of mixed human colonic bacteria in a continuous culture mimicking the human cecal contents. Gastroenterolog *y* **88:**1903–1909.
8. **Elliott, T.** 1992. A method for constructing single-copy *lac* fusions in *Salmonella typhimurium* and its application to the *hemA-prfA* operon. J. Bacteriol. **174:**245–253.
9. **Fasano, A., F. R. Noriega, D. R. Maneval, S. Chanasongcram, S. Russell, S. Guandalini, and M. M. Levine.** 1995. Shigella enterotoxin 1: an enterotoxin of *S. flexneri* 2a active in rabbit small intestine in vivo and in vitro. J. Clin. Investig. **95:**2853–2861.
10. **Fasano, A., F. R. Noriega, F. M. Liao, W. Wang, and M. M. Levine.** 1997. Effect of Shigella enterotoxin 1 (ShET1) on rabbit intestine in vitro and in vivo. Gut **40:**505–511.
11. **Guerrant, R. L., T. S. Steiner, A. A. Lima, and D. A. Bobak.** 1999. How intestinal bacteria cause disease. J. Infect. Dis. **179**(Suppl. 2)**:**S331–337.
12. **Henderson, I. R., J. Czeczulin, C. Eslava, F. Noriega, and J. P. Nataro.** 1999. Characterization of Pic, a secreted protease of *S. flexneri* and enteroaggregative *Escherichia coli*. Infect. Immun. **67:**5587–5596.
13. **Hong, M., Y. Gleason, E. E. Wyckoff, and S. M. Payne.** 1998. Identification of two *S. flexneri* chromosomal loci involved in intercellular spreading. Infect. Immun. **66:**4700–4710.
14. **Jordi, B. J., and C. F. Higgins.** 2000. The downstream regulatory element of the *proU* operon of *Salmonella typhimurium* inhibits open complex formation by RNA polymerase at a distance. J. Biol. Chem. **275:**12123–12128.
15. **Jubete, Y., J. C. Zabala, A. Juarez, and F. de la Cruz.** 1995. *hlyM*, a transcriptional silencer downstream of the promoter in the *hly* operon of *Escherichia coli*. J. Bacteriol. **177:**242–246.
16. **Khan, M. A., and R. E. Isaacson.** 1998. In vivo expression of the β-glucoside (*bgl*) operon of *Escherichia coli* occurs in mouse liver. J. Bacteriol. **180:**4746–4749.
17. **Kotloff, K. L., J. P. Winickoff, B. Ivanoff, J. D. Clemens, D. L. Swerdlow, P. J. Sansonetti, G. K. Adak, and M. M. Levine.** 1999. Global burden of Shigella infections: implications for vaccine development and implementation of control strategies. Bull. WHO **77:**651–666.
18. **Lucht, J. M., P. Dersch, B. Kempf, and E. Bremer.** 1994. Interactions of the nucleoid-associated DNA-binding protein H-NS with the regulatory region of the osmotically controlled *proU* operon of *Escherichia coli*. J. Biol. Chem. **269:**6578–6588.
19. **Maurelli, A. T., R. E. Fernandez, C. A. Bloch, C. K. Rode, and A. Fasano.** 1998. "Black holes" and bacterial pathogenicity: a large genomic deletion that enhances the virulence of *Shigella* spp. and enteroinvasive *Escherichia coli*. Proc. Natl. Acad. Sci. USA **95:**3943–3948.
20. **Miller, J. H.** 1972. Experiments in molecular genetics, p. 356–359. Cold Spring Harbor Laboratory Press, Cold Spring Harbor, N.Y.
21. **Molly, K., M. Vande Woestyne, and W. Verstraete.** 1993. Development of a 5-step multichamber reactor as a simulation of the human intestinal microbial ecosystem. Appl. Microbiol. Biotechnol. **39:**254–258.
22. **Moss, J. E., T. J. Cardozo, A. Zychlinsky, and E. A. Groisman.** 1999. The selC-associated SHI-2 pathogenicity island of *S. flexneri.* Mol. Microbiol. **33:**74–83.
23. **Mukerji, M., and S. Mahadevan.** 1997. Characterization of the negative elements involved in silencing the *bgl* operon of *Escherichia coli*: possible roles for DNA gyrase, H-NS, and CRP-cAMP in regulation. Mol. Microbiol. **24:**617–627.
24. **Murphree, D., B. Froehlich, and J. R. Scott.** 1997. Transcriptional control of genes encoding CS1 pili: negative regulation by a silencer and positive regulation by Rns. J. Bacteriol. **179:**5736–5743.
25. **Nataro, J. P., Y. Deng, S. Cookson, A. Cravioto, S. J. Savarino, L. D. Guers, M. M. Levine, and C. O. Tacket.** 1995. Heterogeneity of enteroaggregative *Escherichia coli* virulence demonstrated in volunteers. J. Infect. Dis. **171:** 465–468.
26. **Nataro, J. P., T. Steiner, and R. L. Guerrant.** 1998. Enteroaggregative *Escherichia coli.* Emerg. Infect. Dis. **4:**251–261.
27. **Overdier, D. G., and L. N. Csonka.** 1992. A transcriptional silencer downstream of the promoter in the osmotically controlled *proU* operon of *Salmonella typhimurium*. Proc. Natl. Acad. Sci. USA **89:**3140–3144.
28. **Sambrook, J., E. F. Fritsch, and T. Maniatis.** 1989. Molecular cloning: a laboratory manual, 2nd ed. Cold Spring Harbor Laboratory Press, Cold Spring Harbor, N.Y.
29. **Schnetz, K.** 1995. Silencing of *Escherichia coli bgl* promoter by flanking sequence elements. EMBO J. **14:**2545–2550.

29a. **Sheikh, J., S. Hicks, M. Dall'Agnol, A. D. Phillips, and J. P. Nataro.** 2001. Roles for Fis and YafK in biofilm formation by enteroaggregative *Escherichia coli*. Mol. Microbiol. **41:**983–997.

30. **Simons, R. W., F. Houman, and N. Kleckner.** 1987. Improved single and multicopy *lac*-based cloning vectors for protein and operon fusions. Gene **53:**85–96.
31. **Steiner, T. S., A. A. Lima, J. P. Nataro, and R. L. Guerrant.** 1998. Enteroaggregative *Escherichia coli* produce intestinal inflammation and growth impairment and cause interleukin-8 release from intestinal epithelial cells. J. Infect. Dis. **177:**88–96.
32. **Summamen, P., E. J. Barron, D. M. Citron, C. A. Strong, H. M. Wexler, and S. M. Finegold.** 1993. Wadsworth anaerobic bacteriology manual, 5th ed., p. 140–146. Star Publishing Co., Belmont, Calif.
33. **Ueguchi, C., and T. Mizuno.** 1993. The *Escherichia coli* nucleoid protein H-NS functions directly as a transcriptional repressor. EMBO J. **12:**1039–1046.
34. **Vokes, S. A., S. A. Reeves, A. G. Torres, and S. M. Payne.** 1999. The aerobactin iron transport system genes in *S. flexneri* are present within a pathogenicity island. Mol. Microbiol. **33:**63–73.
35. **Xu, J., and R. C. Johnson.** 1995. Fis activates the RpoS-dependent stationary-phase expression of *proP* in *Escherichia coli*. J. Bacteriol. **177:**5222–5231.
36. **Xu, J., and R. C. Johnson.** 1995. *aldB*, an RpoS-dependent gene in *Escherichia coli* encoding an aldehyde dehydrogenase that is repressed by Fis and activated by Crp. J. Bacteriol. **177:**3166–3175.
37. **Xu, J., and R. C. Johnson.** 1997. Cyclic AMP receptor protein functions as a repressor of the osmotically inducible promoter *proP* P1 in *Escherichia coli*. J. Bacteriol. **179:**2410–2417.
38. **Yamada, H., T. Yoshida, K. Tanaka, C. Sasakawa, and T. Mizuno.** 1991. Molecular analysis of the *Escherichia coli hns* gene encoding a DNA-binding protein, which preferentially recognizes curved DNA sequences. Mol. Gen. Genet. **230:**332–336.

Editor: D. L. Burns